Influence of ELMs on ICRF wave scattering

W. Zhang[1], T. Y. Xia[2], W. Tierens[1], V. Bobkov[1], J.-M. Noterdaeme[1,3], the ASDEX Upgrade Team[1], and the EUROfusion MST1 Team*

[1]Max-Planck-Institut für Plasmaphysik, Garching, Germany
[2]Institute of Plasma Physics, Chinese Academy of Sciences, Hefei, P. R. China
[3]Applied Physics Department, Ghent University, Gent, Belgium
**see the author list in H. Meyer et al, Nuclear Fusion 57, 102014 (2017)*

Corresponding author: wei.zhang@ipp.mpg.de

ABSTRACT

The influence of ELMs on the propagation of fast wave in the ion cyclotron range of frequency is studied. The 3D edge turbulence code BOUT++ with the Six-field two-fluid model is used to calculate the perturbed density during ELMs, and the antenna code RAPLICASOL is then applied to calculate the antenna fields using the calculated 3D density. The results indicate that ELMs can cause an electric field perturbation in the range of 4.5% - 45% for an ELM induced density perturbation in the range of 3%-30%.

1. INTRODUCTION

The edge localized mode (ELM) is a natural phenomenon of High confinement mode (H-mode) in the edge of tokamak plasmas. It is a disruptive instability likely caused by peeling or ballooning unstable modes [1] and leads to a quasi-periodic relaxation of a transport barrier. During the burst of ELMs, large plasma filaments are injected into the scrape-off layer (SOL), causing large and localized time-varying density and temperature perturbations. These SOL perturbations can however significant influence the propagation of radio frequency (RF) waves. For the electron cyclotron range of frequency waves and lower hybrid waves, it is known from previous studies [2-4] that density turbulence or blobs in the SOL can lead to prominent wave scattering. In this contribution, the influence of ELMs on Ion Cyclotron Range of Frequencies (ICRF) wave fields is investigated for the first time.

In the studies, firstly a simple blob with a Gaussian density distribution is used in a 2D plasma-wave model to calculate its influence on plane wave propagation. This step is important since the realistic ELM density and antenna waves and their interaction are often very complicated. Then the BOUT++ code [5] with the six-field two-fluid model [6] is used to simulate the ELMs with peeling-ballooning modes. The calculated 3D density is used in the 3D antenna code RAPLICASOL (Radiofrequency wAve coupling for Ion Cyclotron Antenna in Scrape-Off-Layer) [7] to calculate the wave fields. In the paper, only the fast wave is considered since the slow wave is evanescent at densities larger than 1e17 m^{-3}. In fact, understanding the perturbation of fast wave fields is most important since it is the one used to heat the main plasma.

2. SIMULATION SETUPS

In the BOUT++ simulations, the EFIT equilibrium of a standard H-mode, #31269 at 3.0s, is used to built a grid with a radial extent of ψ_N= [0.9, 1.2] based on a flux-tube field–aligned coordinate system. Experimental profiles, including the midplane n_e, t_e, n_i, t_i during inter-ELM phases, are used as inputs. The applied Braginskii 6-field two-fluid model [6] solves the evolution of vorticity, ion density, ion temperature, electron temperature, parallel ion velocity as well as perturbed parallel vector potential in 3D realistic geometry [6]. The evolution of ELMs can be well reproduced when the growth of modes reach saturation. An example of the calculated electron density perturbation ($\delta n_e = (n_{e\_ELM} - n_{e0})/n_{e0}$) during an ELM is shown in Fig. 1. Here n_{e0} is the initial unperturbed density and n_{e_ELM} is the perturbed density during an ELM. It is shown that both positive density blobs and negative density holes are developed in the SOL. Their widths are in the order of 10cm/4cm in the poloidal/radial direction; their perturbation magnitudes are in the level of 5%. The calculated 3D perturbed density (n_{e_ELM}) is then transformed in to a slab geometry and used in the RAPLICASOL code with flat antenna model to calculate the wave fields.

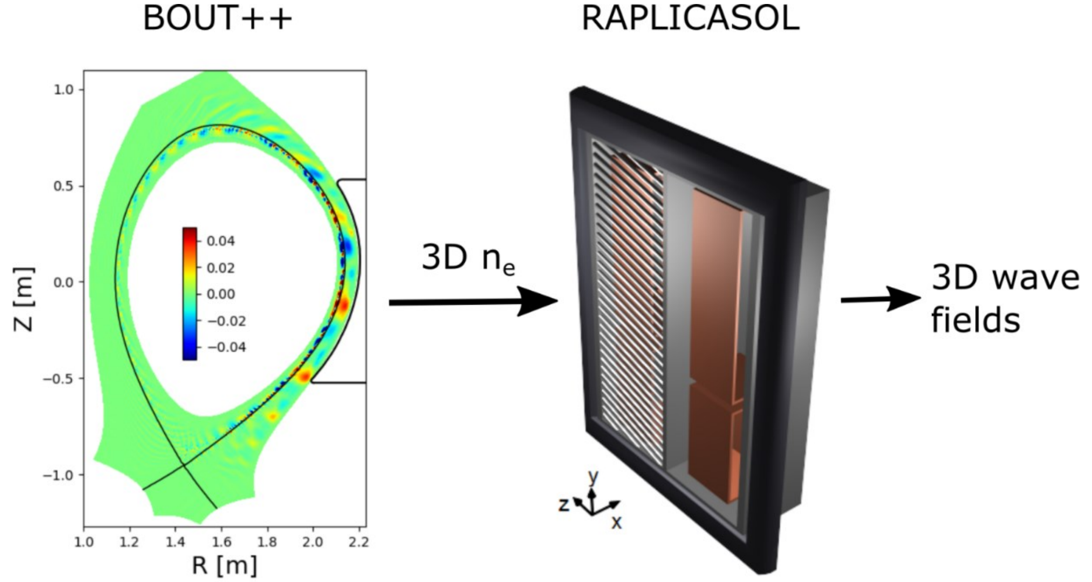

Figure 1. The perturbed electron density calculated by BOUT++ during the burst of an ELM is used in the RAPLICASOL code to calculate the 3D wave fields.

RAPLICASOL is a finite-element solver based on COMSOL. It solves 3D full-wave Maxwell's equations in frequency-domain in the cold plasma approximation in the neighborhood of realistic antenna geometry. A rotated Stix coordinate is used, with (x, y ,z) representing the radial, poloidal and toroidal directions. The background magnetic field lines are set to be parallel to the Faraday screen bars. The simulation region is terminated by an absorbing boundary condition at the core plasma side. By putting a certain amount of power or voltage on the antenna ports, the straps excite waves which then propagate toward the plasma core. In our simulations, the benchmarked flat antenna model [7] is used (Fig. 1). Since the density at the leading edge of antenna limiters is ~3.3e17 m^{-3}, the slow wave does not propagate at and beyond this density and is thus not considered in our study. A vacuum layer with a width of 6 cm is setup in front of the straps in order to avoid the Lower Hybrid Resonance layer of slow wave. Besides the 3D density, other important parameter settings in RAPLICASOL include: 1 volt at each port; ICRF heating frequency f_{ICRF}= 36.5 MHz; central magnetic field B_0 = -2.5 T; 5% Hydrogen minority in the bulk Deuterium plasma; radial, poloidal and toroidal extension of the simulated region are 0.36 m, 1.86m, 2.23 m, respectively.

3. SIMULATION RESULTS

Because of the complexity of wave scattering by ELMs, it is very important to first understand the scattering of fast wave by a single density blob. A 2D COMSOL model (Fig. 2, top) calculating the Radio-Frequency plane waves in Plasma (RFP) has been built [8]. The wave is excited by a line current on the right boundary of the simulation domain. A Perfect Matching Layer (PML) is set on the left boundary while a periodic boundary condition is set at the top and bottom boundaries. The blob is assumed to have a Gaussian density distribution, with its center at (x_0, y_0)=(0, 0), maximum value of δn_{e_max}=0.1 and standard deviation of σ_x=σ_y=0.02. The background density is homogeneously equal to n_{e0}=5e19 m^{-3}. The slow wave is ignored since it is evanescent for density larger than 5e16 m^{-3}. The magnetic field B_0 is in the z direction.

The calculated relative change of $|E_y|$ is expressed as $\delta|E_y| = (|E_{y\_per}| - |E_{y0}|)/|E_{y0}|$, in which E_{y0} and E_{y_per} are the y component of electric field with unperturbed and perturbed density, respectively. The same calculation is done for $\delta|E_x|$. The results (Fig. 2, bottom) show that for a blob with a density perturbation of 10%, it can cause $|E_y|$ perturbation in the level of 15% and a $|E_x|$ perturbation in the level of 10%. Both increase and decrease of electric fields are seen within the blob, and the modifications of the $|E_y|$ and $|E_x|$ inside the blob are usually the largest. It should be noted that modification of electric field also exists outside of the blob, indicating that the modification of electric field is more a global effect. Changes in the left side of the blob are due to wave scattering while changes in the right side are likely due to wave reflection by the blob. A scattering cone in the direction of wave propagation can often be recognized.

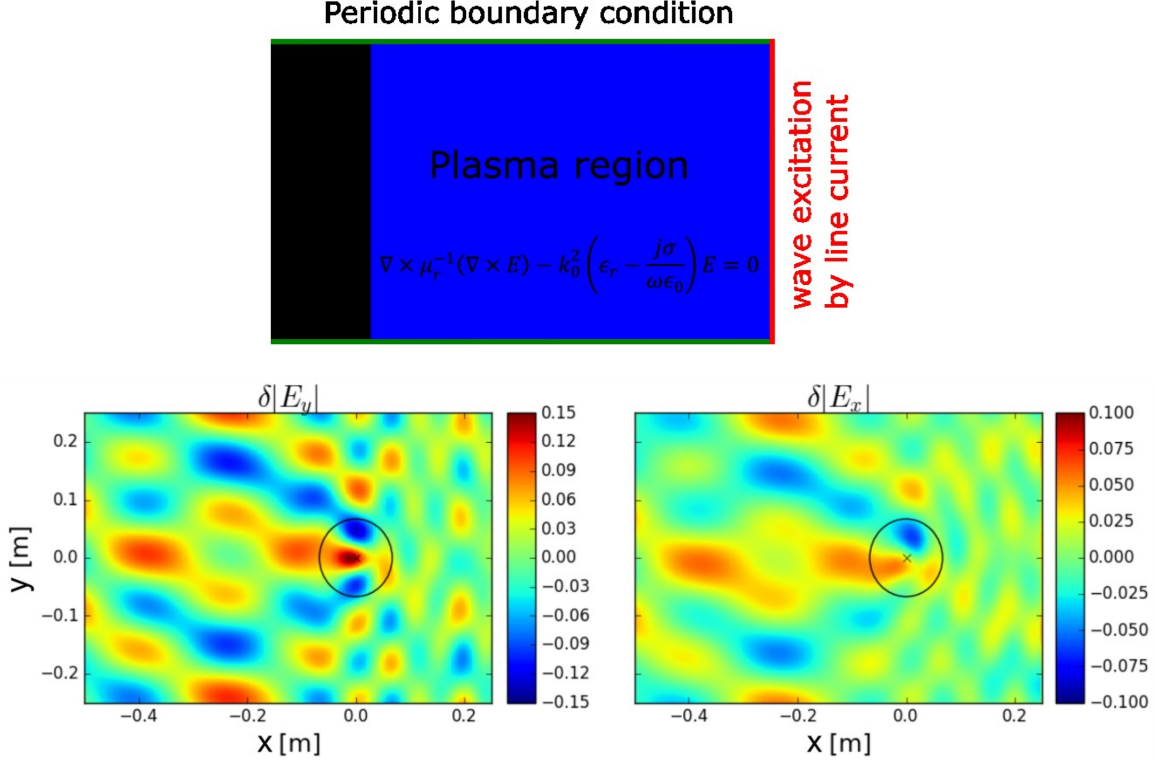

Figure 2. Top: schematic view of the 2D COMSOL model. Bottom: relative changes of $|E_y|$ and $|E_x|$ fields by a blob. The black circles in the figure represent the boundary of blobs.

Then, RAPLICASOL simulations using 3D density calculated by BOUT++ are performed. The parallel wave number of the power spectrum is $k_{\parallel} \approx 9\ m^{-1}$, according to the fast wave dispersion relation, we get $k_{\perp} \approx 49.2\ m^{-1}$ and $\lambda_{\perp} \approx 0.13\ m$. In our simulations, the ELM filamentary size in the radial and poloidal direction can be as large as 0.02m and 0.1m. The size in the poloidal direction can be comparable to the wavelength.

The results of interest are shown in Fig. 3. It is shown that for the considered density perturbation in the level of 3%, $\delta|E_y|$ is in the range 3%-5% while $\delta|E_x|$ is in the range of 2%-3%. E_Z is not considered since $|E_Z| \ll |E_x| \sim |E_y|$ for the studied plasma which has $\mathrm{n_{e\_edge}} \sim 1.0\mathrm{e}19\ m^{-3}$. The changes of $\delta|E_y|$ and $\delta|E_x|$ not only exist in the SOL but also occur inside the seperatrix. It should be noted that a density hole can cause both increase and decrease of electric field. Moreover, as a local electric field can be influenced by multiple density blobs and holes, the change of electric field can become very complex because ELMs induce multiple density blobs and holes in the SOL. Thus, it is hard to identify whether the electric field in a certain location will be increased or decreased. Nevertheless, it can still be pointed out that the largest contribution to a local modification of electric field should come from the largest density perturbations nearby. The scattering cone, usually seen in the case of one density blob, is hardly visible in the case of multiple density blobs and holes.

Further parameter scan studies show that the electric field perturbations depend almost linearly on the density perturbations. For a density perturbation in the range 3% - 30%, the calculated $\delta|E_y|$ value ranges between 4.5%-45%. This indicates that for scenarios with big ELMs, the scattering of fast wave can become significant.

The changing of the SOL density by ELM filaments will change the ICRF coupling and ICRF heating efficiency, which has been observed in previous experiments [9]. It is expected that the ICRF coupling can be increased, as the ELMs flatten the pedestal and pump out part of the density into the far SOL, making the antenna - cut off density distance becomes smaller. On the other hand, the scattering of the fast wave and the changing of the wave fields by the ELM filaments can result in less RF power reaching the resonance layer, where the ICRF wave energy is supposed to be absorbed by the core plasma. Further calculations are planned in the near future to understand the influence of ELMs on ICRF coupling and ICRF heating efficiency.

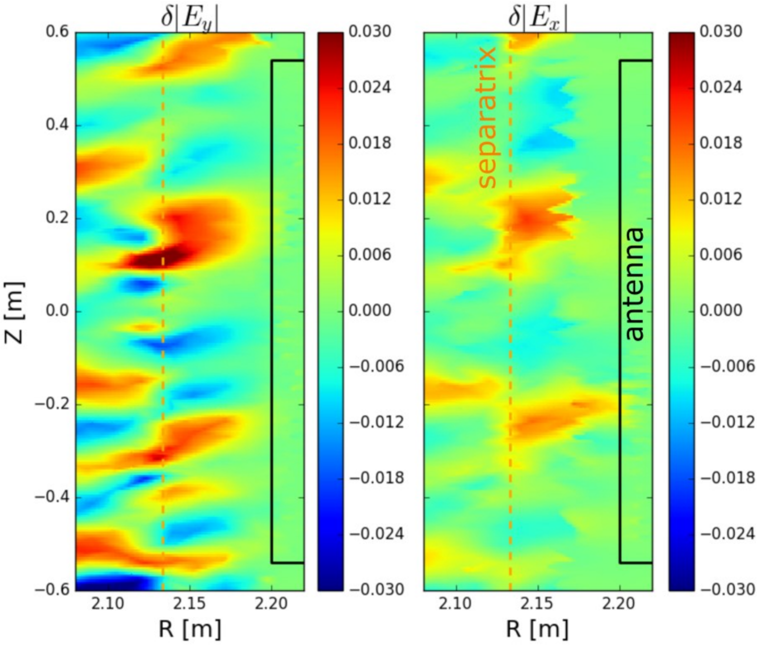

Figure 3. Relative changes of $|E_y|$ and $|E_x|$ during an ELM. They are calculated with the strategies in figure 1.

4. CONCLUSIONS

The scattering of fast wave in the ion cyclotron range of frequency by ELMs has been studied. The edge turbulence code BOUT++ is used to calculate the scrape-off layer density during ELMs, and the antenna code RAPLICASOL is used to calculate the electric fields. It is shown that a density blob or a density hole can cause localized increase and decrease of electric fields, and this modification is usually a global effect. A scattering cone, starting from the center of the blob, can often occur in the direction of wave propagation. The structure of the electric field perturbation caused by multiple density blobs and holes can be very complex, while the perturbation magnitude depends on the perturbation magnitude of the density. An ELM with a density perturbation in the level of 3% can lead to an electric field perturbation in the level of 4.5%, while a density perturbation in the level of 30% can lead to an electric field perturbation in the level of 45%. Thus, the modifications of electric fields can be prominent during a large ELM.

More quantitative calculations are ongoing, such as parameter scans, power scattering ratio and evolution of the electric fields during an ELM. In addition, the 3D curved antenna model [10] will be used in our future calculations once it is benchmarked.

ACKNOWLEDGMENTS

This work has been carried out within the framework of the EUROfusion Consortium and has received funding from the Euratom research and training programme 2014-2018 and 2019-2020 under grant agreement No 633053. The views and opinions expressed herein do not necessarily reflect those of the European Commission.

[1] Snyder P. B. *et al* 2002 *Physics of Plasmas* **9** 2037-43
[2] Myra J. R. *et al* 2010 *Physics of Plasmas* **17** 102510
[3] Snicker A. *et al* 2018 *Nuclear Fusion* **58** 016002
[4] Ram A. K. *et al* 2016 *Physics of Plasmas* **23** 022504
[5] Dudson B. D. *et al* 2009 *Computer Physics Communications* **180** 1467-80
[6] Xia T. Y. *et al* 2013 *Nuclear Fusion* **53** 073009
[7] Jacquot J. *et al* 2015 *AIP Conference Proceedings* **1689** 050008
[8] Zhang W. *et al* 2019 *"Scattering of fast wave by blobs and ELMs" to be submitted*
[9] Bobkov V. *et al* "Interaction of ICRF electric fields and the SOL plasma in ASDEX Upgrade" *30th EPS Conference on Controlled Fusion and Plasma Physics (St. Petersburg, 2003)* 27A P-1.165
[10] Tierens W. *et al* 2019 *"Recent improvements to the ICRF antenna coupling code RAPLICASOL", this conference*